Ultra-thin titanium oxide

M. Bareiß,[1,a)] D. Kälblein,[2] C. Jirauschek,[1] A. Exner,[1] I. Pavlichenko,[3] B. Lotsch,[3] U. Zschieschang,[2] H. Klauk,[2] G. Scarpa,[1] B. Fabel,[1] W. Porod,[4] and P. Lugli[1]
[1]*Institute for Nanoelectronics, Technische Universität München, Munich, Germany*
[2]*Max Planck Institute for Solid State Research, Stuttgart, Germany*
[3]*Department of Chemistry, Ludwig-Maximilians-Universität, Munich, Germany*
[4]*Center for Nano Science and Technology, University of Notre Dame, Notre Dame, Indiana 46556, USA*

(Received 20 June 2012; accepted 30 July 2012; published online 23 August 2012)

We demonstrate the fabrication of ultra-thin titanium oxide films by plasma-induced surface oxidation. Ellipsometry measurements indicate an oxide thickness of about 2 nm. Electrical characterization was performed on microscale and nanoscale metal-insulator-metal tunneling diodes. Electrical fields up to 22 MV/cm were applied without destroying the titanium oxide films. The current-voltage-characteristic of the diodes are found to be asymmetric with respect to zero bias when employing electrodes with different work functions. The permittivity of the ultra-thin titanium oxide was determined to be less than 6, which is the smallest permittivity that has been reported for titanium oxide. © *2012 American Institute of Physics*. [http://dx.doi.org/10.1063/1.4745651]

Thin films of titanium oxide (TiO_x) are potentially useful for various applications, such as solid-state memory cells,[1] memristors,[2] gate insulators in field-effect transistors,[3] solar cells,[4] or photochemical applications.[5] In addition, thin dielectric films have been found to be useful for high-frequency electronic applications, such as metal-insulator-metal (MIM) tunneling diodes.[6–9] In a MIM tunneling diode, charge carriers tunnel between two metal electrodes through the thin insulator. Tunneling occurs in both directions, but by choosing metal electrodes with different work functions, the magnitude of the tunneling current will be larger in one direction than in the other direction. This effect can be exploited for the rectification of alternating currents at very high frequencies, even in the terahertz (THz) regime.[10] In our previous work,[11] aluminum oxide (AlO_x) was employed as the tunneling dielectric. However, AlO_x has a large bandgap. In order to generate a larger electrical signal from the diode (i.e., larger tunneling currents through the insulator), a smaller bandgap dielectric is required. A promising candidate is TiO_x. One drawback of TiO_x for this application is that the permittivity of TiO_x is reported to be relatively large,[12] which would in turn lead to a large capacitance and hence to a small cut-off frequency of the MIM diodes.[13] We have recently observed that the permittivity of thin AlO_x dielectrics decreases with decreasing dielectric thickness. Assuming this effect occurs in TiO_x as well, very thin TiO_x films are potentially useful for MIM tunneling diodes with large current signal (due to the small bandgap) and high cut-off frequency (due to the small permittivity).

TiO_x layers with thicknesses of less than 10 nm can be fabricated by a variety of techniques, such as (plasma-enhanced) chemical vapor deposition,[1] sputtering,[3] and atomic layer deposition.[14] It is however challenging to produce large areas films of pure titanium oxide with good homogeneity when the film thickness is in the range of a few nanometers. We present here a fabrication method for titanium oxide resulting in an ultra-thin dielectric with a thickness of about 2 nm over large areas. The thickness of the oxide was determined by ellipsometry. For electrical measurements, two metal electrodes with dissimilar work functions (Ti and Au) were prepared. Electrical measurements on microscale diodes and of ensembles of nanoscale diodes were carried out. Direct tunneling was observed, and static parameters were determined by fitting a numerical model to the experimental data. The permittivity of these ultra-thin oxide films determined from capacitance measurements indicates that the permittivity indeed strongly depends on the thickness of the insulator. Nanoscale crossbar structures were fabricated in a two-step nanotransfer printing (nTP) process. In this way, thousands of rectifying diodes can be fabricated that are expected to have cut-off frequencies in the terahertz range.

In order to fabricate microscale MIM diodes, a metal electrode (Ti) was deposited through a shadow mask featuring line-like openings onto a silicon wafer covered by a 100-nm-thick layer of thermally grown silicon dioxide. To produce the ultra-thin TiO_x dielectric, the surface of the Ti layer was oxidized in an Oxford Plasma Technology Reactive Ion Etch (RIE) system operated at an oxygen partial pressure of 10 mTorr and a plasma power of 200 W for 30 s. These parameters are similar to those previously used for the fabrication of thin aluminum oxide layers.[15,16] The second metal electrode (Au) was deposited perpendicular to the other electrode by thermal evaporation through a second shadow mask featuring line-like openings as well. In this way, an array of Ti-TiO_x-Au crossbar structures was fabricated that allows each individual diode to be contacted with probe needles outside of the active area without damaging the dielectric.

The nanoscale MIM diodes were fabricated by nTP.[17] A silicon stamp was prepared by etching trenches into the surface of a silicon wafer using a combination of electron-beam lithography and dry etching to produce raised, 100-nm-wide lines. The silicon was then covered with an alkylsilane self-assembled monolayer (SAM) in order to render the stamp surface hydrophobic (Fig. 1(a)). A 25-nm-thick Au followed by 4-nm-thick Ti was deposited onto the SAM-covered silicon stamp by thermal evaporation. Since Au is a noble metal

[a)]Author to whom correspondence should be addressed. Electronic mail: Bareiss@nano.ei.tum.de.

 © 2012 American Institute of Physics

Downloaded 27 Aug 2012 to 134.105.227.101. Redistribution subject to AIP license or copyright; see http://apl.aip.org/about/rights_and_permissions

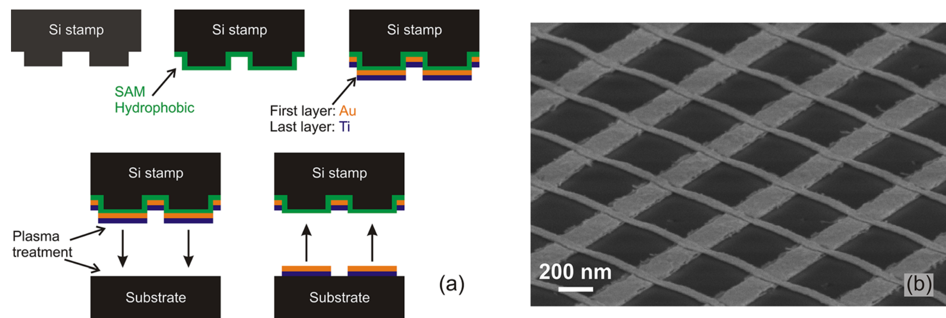

FIG. 1. (a) nTP process: A stamp is covered with a hydrophobic alkylsilane SAM and a stack of two metals is then deposited thereon. The surfaces of the stamp and of the target substrate (glass) are activated by oxygen-plasma treatments and then brought into physical contact, causing the metal stack to be transferred from the raised regions of the stamp onto the target substrate. (b) Scanning electron microscopy (SEM) image of a crossbar array fabricated in a two-step nTP process. The width of the bottom lines is 100 nm, which of the top lines is 50 nm.

and the stamp surface is hydrophobic, the adhesion of the metal stack on the stamp surface is sufficiently weak to facilitate delamination of the metal stack during stamping. The 25-nm-thick Au layer later serves as the bottom electrode of the nanoscale MIM diodes. The 4-nm-thick Ti layer serves as an adhesion promoter to facilitate the transfer of the metal stack from the stamp onto the target substrate during stamping. To further improve the adhesion of the metal stack on the target surface, the Ti was activated by a brief oxygen-plasma treatment that increases the density of hydrophilic hydroxyl groups. The density of siloxane groups on the surface of the target substrate (glass) was increased in the same manner. After these two activation steps, the stamp was brought into physical contact with the target substrate, and a pressure of 50 bars and a temperature of 200 °C were applied for 3 min. This causes the metals to be transferred from the raised regions of the stamp onto the glass substrate. Onto a second silicon stamp that was prepared similar to the other one (i.e., by covering the surface with raised, 50 nm-wide lines and rendering it hydrophobic with a SAM), 25-nm-thick Au followed by 25-nm-thick Ti were deposited by thermal evaporation. The 25-nm-thick Ti layer later serves as the top electrode of the nanoscale MIM diodes. The ultra-thin TiO_x dielectric was then produced by oxidizing the Ti surface in the same way as described above for the microscale MIM diodes. Finally, the Au-Ti-TiO_x stack was transfer-printed onto the target substrate in an orientation perpendicular with respect to the previously patterned Ti-Au lines, resulting in a dense array of Ti-Au-TiO_x-Ti-Au crossbar structures (Fig. 1(b)). To allow electrical characterization of the nanoscale MIM diodes, contact pads were fabricated by photolithography, metal deposition, and lift-off.

For ellipsometry measurements, a 30-nm-thick layer of Ti was deposited by thermal evaporation onto a silicon wafer covered with thermally grown silicon dioxide. The Ti surface was then oxidized by oxygen plasma as described above, and ellipsometry was performed to determine the oxide thickness.

The thickness of the plasma-grown TiO_x was determined by ellipsometry. The angle of incidence was varied between 65° and 75° with respect to the surface normal, and several measurements were performed. By fitting the experimental data to the Cauchy relationship,[18] an oxide thickness of 2.0 nm ± 0.02 nm was calculated (see Fig. 2). Since a loss feature in TiO_x around 300 nm occurs,[19] we fit the experimental data between 400 nm and 900 nm in which the Cauchy model is valid.[20] The mean square error in this fit is 1.087 and the refractive index determined from the fit is 2.04 at 550 nm.

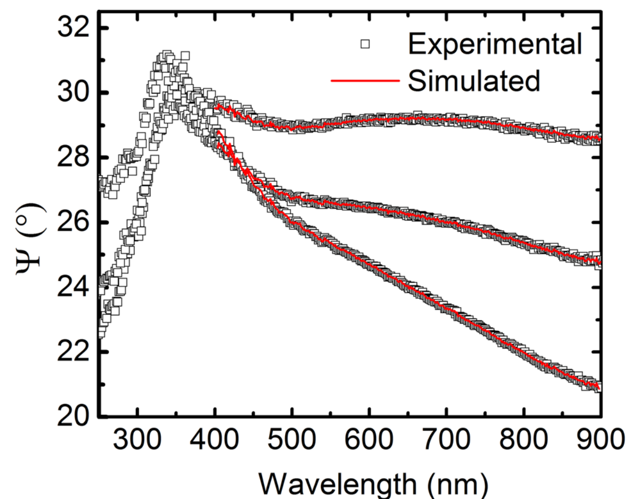

FIG. 2. Measured (black squares) and simulated (red lines) ellipsometric spectra of ultra-thin (~2.0 nm) plasma-grown titanium oxide films at three different angles of incidence (65°, 70°, and 75°). By fitting the measurement data to the Cauchy model, the oxide thickness was calculated.

The permittivity of these ultra-thin TiO_x films was determined by measuring the capacitance of several microscale Ti-TiO_x-Au diodes. The Ti bottom electrode was set to ground potential and a DC potential modulated with a small AC bias was applied to the Au top electrode. An average capacitance per unit area of $2.25 \cdot 10^{-6}$ F/cm^2 was calculated. This corresponds to a permittivity of 5.1 when assuming an oxide thickness of 2.0 nm (as determined by ellipsometry). This is the smallest permittivity that has been reported for titanium oxide (Table I).

TABLE. I. Permittivity of titanium oxide reported in the literature and determined in this work.

Method	Thickness (nm)	Permittivity
CVD (Ref. 26)	~7–90	7–55
PECVD (Ref. 1)	20~200	~60
Sputtered (Ref. 3)	10	95
Sputtered (Ref. 27)	300~500	50~70
ALD (Ref. 14)	9–25	60–80
ALD (Ref. 28)	35–140	60–100
Plasma (this work)	2	5.1

Downloaded 27 Aug 2012 to 134.105.227.101. Redistribution subject to AIP license or copyright; see http://apl.aip.org/about/rights_and_permissions

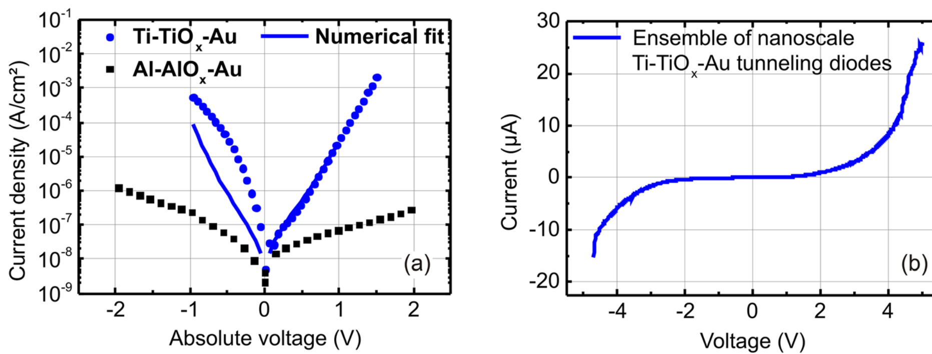

FIG. 3. (a) Measured (blue circles) and simulated (blue lines) current-voltage characteristics of a shadow-mask-patterned microscale Ti-TiOx-Au and Al-AlOx-Au (black squares) tunneling diode. (b) Measured current-voltage-characteristics of an ensemble of transfer-printed nanoscale Au-TiOx-Ti tunneling diodes.

The current-voltage-characteristics of individual shadow-mask-patterned microscale Ti-TiO_x-Au diodes were measured in ambient air via a semiconductor parameter analyzer at room temperature by contacting the metal electrodes outside of the active area using probe needles. In these measurements, the Ti bottom electrode was set to ground potential, and a positive or negative potential was applied to the Au top electrode. The current through the diodes was measured as a function of the applied voltage. The results are shown in Figure 3(a). The circles represent the experimental data obtained from the Ti-TiO_x-Au diodes. In the graph, the absolute value of the current density is plotted as a function of the applied voltage, so that the asymmetry of the current-voltage curves can be easily evaluated. For comparison, the measured current-voltage characteristics of a previously fabricated Al-AlO_x-Au tunneling diode[17] are also shown (squares).

As can be seen in Figure 3(a), the current-voltage characteristics of the MIM diodes are asymmetric around zero bias. For example, at an applied voltage of -0.5 V, the absolute value of the current density is two orders of magnitude larger than the current density at $+0.5$ V. More importantly, the observed degree of asymmetry is much larger in the Ti-TiO_x-Au diodes than in the Al-AlO_x-Au diodes. In order to identify the mechanism of charge transport through the ultra-thin titanium oxide films, numerical simulations[21] were carried out. The work functions of Ti and Au were assumed to be 3.95 eV and 5.2 eV,[22] respectively, and the thickness of the TiO_x was assumed to be to 2.0 nm (as indicated by the ellipsometry measurements). The effective mass of the electrons tunneling through the dielectric and the height of the potential barrier at the Ti/TiO_x interface were adjusted until a satisfactory fit to the experimental data was obtained. We determined an effective electron mass in TiO_x of $m_{ox} = 2.62 \cdot m_e$ and a barrier height at the Ti/TiO_x interface of 0.71 eV, in good agreement with literature.[23,24] In Figure 3(a), this numerical fit is shown with blue lines. We believe that the observed discrepancy between the experimental data and the numerical fit for negative voltages is due to the presence of interfacial traps that reduce the effective potential barrier height until the traps are depleted.[25] For the most part, the numerical model provides a satisfactory fit of the experimental data, showing that direct tunneling is the main conduction mechanism.

In addition to individual shadow-mask-patterned microscale Ti-TiO_x-Au tunneling diodes, we also measured the current-voltage characteristics of an ensemble of transfer-printed nanoscale Au-TiO_x-Ti tunneling diodes. All diodes within this ensemble are connected in parallel (see Figure 1(b)). The exact number of functional diodes within the ensemble is unknown, since some fraction of the diodes are believed to be short-circuited (which also produces a finite shunt resistance). The measured current-voltage characteristics of the ensemble are shown in Figure 3(b). As can be seen, the dependence of the measured current on the applied voltage is exponential as well as asymmetric with respect to the zero bias.

We have reported on a fabrication method to produce ultra-thin titanium oxide films by an oxygen plasma. The materials characteristics, such as the thickness and the permittivity of the TiO_x films, were determined by ellipsometry and by capacitance measurements. Since electric fields up to 22 MV/cm can be applied without damaging the dielectric, this method is suitable for the fabrication of high-quality insulating films. The current density through these ultra-thin titanium oxide films is 4 orders of magnitude larger than the current density previously measured in thin films of plasma-grown AlO_x. The permittivity of the ultra-thin titanium oxide films was found to be much smaller than the permittivity of thicker titanium oxide films, which means that the ultra-thin TiO_x is an excellent candidate for rectifying metal-insulator-metal tunneling diodes in terahertz applications, such as infrared detectors.

The authors thank Margarete Remm and IMS Chips for their outstanding support. The research leading to these results has received funding from the Institute for Advanced Study (IAS) and the International Graduate School for Science and Engineering (IGSSE) of the Technische Universität München and by the German Excellence Cluster "Nanosystem Initiative Munich" (NIM).

[1] Y. H. Lee, K. K. Chan, and M. J. Brady, J. Vac. Sci.Technol. A **13**, 596–601 (1995).
[2] A. S. Alexandrov, A. M. Bratkovsky, B. Bridle, S. E. Savel'ev, D. B. Strukov, and R. S. Williams, Appl. Phys. Lett. **99**, 202104 (2011).
[3] B. H. Lee, Y. Jeon, K. Zawadzki, W.-J. Qi, and J. Lee, Appl. Phys. Lett. **74**, 3143–3145 (1999).
[4] U. Bach, D. Lupo, P. Comte, J. E. Moser, F. Weissürtel, J. Salbeck, H. Spreitzer, and M. Grätzel, Nature (London) **395**, 583–585 (1998).
[5] S. U. M. Khan, M. Al-Shahry, and W. B. Ingler, Jr., Science **297**, 2243–2245 (2002).
[6] M. Bareiß, B. N. Tiwari, A. Hochmeister, G. Jegert, U. Zschieschang, H. Klauk, B. Fabel, G. Scarpa, G. Koblmüller, G. H. Bernstein, W. Porod, and P. Lugli, IEEE Trans. Microwave Theory Tech. **59**, 2751–2757 (2011).
[7] J. A. Bean, B. Tiwari, G. H. Bernstein, P. Fay, and W. Porod, J. Vac. Sci. Technol. B **27**, 11–14 (2009).
[8] C. Fumeaux, G. D. Boreman, W. Herrmann, F. K. Kneubühl, and H. Rothuizen, Appl. Opt. **38**, 37–46 (1999).

Downloaded 27 Aug 2012 to 134.105.227.101. Redistribution subject to AIP license or copyright; see http://apl.aip.org/about/rights_and_permissions

[9]S. Grover and G. Moddel, Solid-State Electron. **67**, 94–99 (2012).
[10]J. A. Bean, A. Weeks, and G. D. Boreman, IEEE J. Quantum Electron. **47**, 126–135 (2011).
[11]M. Bareiß, A. Hochmeister, G. Jegert, U. Zschieschang, H. Klauk, R. Huber, D. Grundler, W. Porod, B. Fabel, G. Scarpa, and P. Lugli, J. Appl. Phys. **110**, 044316 (2011).
[12]J. Robertson, Rep. Prog. Phys. **69**, 327–396 (2005).
[13]M. Bareiß, F. Ante, D. Kälblein, G. Jegert, C. Jirauschek, G. Scarpa, B. Fabel, E. M. Nelson, G. Timp, U. Zschieschang, H. Klauk, W. Porod, and P. Lugli, ACS Nano **6**, 2853–2859 (2012).
[14]S. K. Kim, S. Y. Lee, M. Seo, G.-J. Choi, and C. S. Hwang, J. Appl. Phys. **102**, 024109 (2007).
[15]H. Klauk, U. Zschieschang, J. Pflaum, and M. Halik, Nature (London) **445**, 745 (2007).
[16]T. Sekitani, U. Zschieschang, H. Klauk, and T. Someya, Nature Mater. **9**, 1015–1022 (2010).
[17]S. Kim, A. Carlson, H. Cheng, S. Lee, J.-K. Park, Y. Huang, and J. A. Rogers, Appl. Phys. Lett. **100**, 171909 (2012).
[18]H. G. Tompkins, T. Zhu, and E. Chen, J. Vac. Sci. Technol. A **16**, 1297–1302 (1998).
[19]D. Yugang, Z. Yuan, T. Yiping, and L. Dichen, Rapid Prototyping J. **17**, 247–252 (2011).
[20]J. N. Hilfiker, N. Singh, T. Tiwald, D. Convey, S. M. Smith, J. H. Baker, and H. G. Tompkins, Thin Solid Films **45**, 7979–7989 (2008).
[21]C. Jirauschek, IEEE J. Quantum Electron. **45**, 1059–1067 (2009).
[22]M. Irimia-Vladu, E. D. Glowacki, P. A. Troshin, G. Schwabegger, L. Leonat, D. K. Susarowa, O. Krystal, M. Ullah, Y. Kanbur, M. A. Bodea, V. F. Razumov, H. Sitter, S. Bauer, and N. S. Sariciftci, Adv. Mater. **24**, 375–380 (2011).
[23]S. X. Zhang, D. C. Kundaliya, W. Yu, S. Dhar, S. Y. Young, L. G. Salamanca-Riba, S. B. Ogale, R. D. Vispute, and T. Venkatesan, J. Appl. Phys. **102**, 013701 (2007).
[24]Y.-H. Chang, C.-M. Liu, Y.-C. Tseng, C. Chen, C.-C. Chen, and H.-E. Cheng, Nanotechnology **21**, 225602 (2010).
[25]D. J. Dumin, S. K. Mopuri, S. Vanchinathan, R. S. Scott, R. Subramomiam, and T. G. Lewis, IEEE Trans. Electron Devices **42**, 760–772 (1995).
[26]N. Rausch and E. P. Burte, Microelectron. Eng. **19**, 725–728 (1992).
[27]M. D. Stamate, Thin Solid Films **372**, 246–249 (2000).
[28]Q. Xie and Y.-L. Jiang, J. Appl. Phys. **102**, 083521 (2007).

Downloaded 27 Aug 2012 to 134.105.227.101. Redistribution subject to AIP license or copyright; see http://apl.aip.org/about/rights_and_permissions